minerals

MDPI

Article

X-ray Diffraction Phase Analysis of Changes in the Lattice of Pervouralsk Quartzite upon Heating

Viktor Alekseevich Kukartsev [1], Aleksandr Ivanovich Cherepanov [1], Vladislav Viktorovich Kukartsev [2,3], Vadim Sergeevich Tynchenko [4,5,6,*], Vladimir Viktorovich Bukhtoyarov [5,6,7], Aleksei Mikhailovich Popov [8], Roman Borisovich Sergienko [9] and Sergei Vasilievich Tynchenko [10,11]

1 Department of Materials Science and Materials Processing Technology, Polytechnical Institute, Siberian Federal University, 660041 Krasnoyarsk, Russia; vkukarstev@sfu-kras.ru (V.A.K.); acherepanov@sfu-kras.ru (A.I.C.)
2 Department of Informatics, Institute of Space and Information Technologies, Siberian Federal University, 660041 Krasnoyarsk, Russia; vlad_saa_2000@mail.ru
3 Department of Information Economic Systems, Institute of Engineering and Economics, Reshetnev Siberian State University of Science and Technology, 660037 Krasnoyarsk, Russia
4 Information-Control Systems Department, Institute of Computer Science and Telecommunications, Reshetnev Siberian State University of Science and Technology, 660037 Krasnoyarsk, Russia
5 Department of Technological Machines and Equipment of Oil and Gas Complex, School of Petroleum and Natural Gas Engineering, Siberian Federal University, 660041 Krasnoyarsk, Russia; vladber@list.ru
6 Digital Material Science: New Materials and Technologies, Bauman Moscow State Technical University, 105005 Moscow, Russia
7 Department of Information Technology Security, Reshetnev Siberian State University of Science and Technology, 660037 Krasnoyarsk, Russia
8 Institute of Informatics and Telecommunications, Reshetnev Siberian State University of Science and Technology, 660037 Krasnoyarsk, Russia; vm_popov@sibsau.ru
9 Machine Learning Department, Gini Gmbh, 80339 Munich, Germany; roman@gini.net
10 Department of Digital Control Technologies, Institute of Business Process Management, Siberian Federal University, 660041 Krasnoyarsk, Russia; 051311@mail.ru
11 Department of Computer Science and Computer Engineering, Institute of Computer Science and Telecommunications, Reshetnev Siberian State University of Science and Technology, 660037 Krasnoyarsk, Russia
* Correspondence: vadimond@mail.ru; Tel.: +7-95-0973-0264

check for updates

Citation: Kukartsev, V.A.; Cherepanov, A.I.; Kukartsev, V.V.; Tynchenko, V.S.; Bukhtoyarov, V.V.; Popov, A.M.; Sergienko, R.B.; Tynchenko, S.V. X-ray Diffraction Phase Analysis of Changes in the Lattice of Pervouralsk Quartzite upon Heating. *Minerals* **2022**, *12*, 233. https://doi.org/10.3390/min12020233

Academic Editor: Olivier Proux

Received: 20 December 2021
Accepted: 9 February 2022
Published: 11 February 2022

Publisher's Note: MDPI stays neutral with regard to jurisdictional claims in published maps and institutional affiliations.

Copyright: © 2022 by the authors. Licensee MDPI, Basel, Switzerland. This article is an open access article distributed under the terms and conditions of the Creative Commons Attribution (CC BY) license (https://creativecommons.org/licenses/by/4.0/).

Abstract: At present, quartzite is widely used across many industries. The properties of quartzite significantly affect the technology used during the preparation of the raw materials as well as the technology used for manufacturing the final product, which may be intended for further operation at different temperatures. The purpose of the study was to create a scheme for the transformation of quartzite that would describe the changes in the parameters of its lattice parameter upon heating and would offer guidance regarding the drying technology and technology required to obtain tridymite. A Bruker D8 Advance diffractometer was used to study changes in the phase composition of quartzite at the temperatures of 200, 400, 600, 879, 1000, 1200, 1470, and 1550 °C. A detailed scheme of transformations of PKMVI-1 quartzite with a SiO_2 content of at least 97.5% at normal pressure was proposed for crystalline modifications formed during its heating. As a result of this research, the changes in the parameters of the lattice parameter—such as the average interplanar distance d_{avg}, the volume of the unit cell V_{avg}, the density of the unit cell D_{avg}, and the molecular weight M_{avg}—were established.

Keywords: quartzite; lattice parameter; interplanar spacing; X-ray phase analysis; refractory material; cell volume

1. Introduction

The modern economy is focused on innovative development; therefore, it stimulates the creation of promising new materials and technological processes. Increased require-

ments are imposed on the developed technological processes since they must ensure the production of high-quality raw materials that will allow them to be used in harsh conditions—such as extreme temperatures, aggressive chemical and radiation environments, under high mechanical loads, etc. [1]. Research in advanced physicochemical methods examines the behavior of these materials under their expected operational conditions, the optimal method for their synthesis, and the relationship between their properties and their atomic and molecular structures.

Manufacturers and consumers of refractory materials must adhere to highly technical production requirements due to the demand for increased thermal performance as a result of the introduction of progressive high-temperature processes. For this reason, the level of refractoriness, wear resistance, and the service life of a material—especially at higher temperatures (e.g., for quartzite and refractory products and materials made from it, this is 1600–1670 °C)—must increase [2].

In 1912, Fenner used physicochemical analysis to observe the changes that occurred in quartzite during the heating process, and since that time, researchers in the field have been guided by his diagrams [3]. Later, in 1971, Pryanishnikov carried out similar studies using the X-ray method and a modified scheme of quartzite transformations during heating was proposed, in which the crystalline modification of tridymite was absent [4]. When developing the technology for smelting synthetic iron in induction furnaces for industrial use, a lining of quartzite was used because, under high temperatures, it would form tridymite, which was a more stable modification to withstand extreme heating. In the 1980s, the durability of such a lining reached around 350–400 heats, but since the late 1990s, a sharp decrease in its durability has been noted [5]. Therefore, scientists studied the changes in the lattice parameter of quartzite during heating, using modern, structural X-ray analysis. A sampling of these studies is presented in [6–8]. This research made it possible to establish new technological regimes for the preparation of quartzite lining that would improve its durability. The present study centered on developing an accurate, consistent preparation for the stable transformation of Pervouralsk quartzite, which is typically used for the lining of induction crucible furnaces.

Information on the elemental composition of various objects (e.g., rocks, minerals, chemical compounds, alloys, etc.) can be obtained using a variety of analytical methods, often involving the destruction of the matter. Complex substances, formed as a result of the combination of chemical elements, number in the hundreds of thousands. These complex substances have a variety of properties as a result of the differences in their chemical compositions and their mutual arrangements of atoms (i.e., their structures) [8]. Only diffraction methods (e.g., X-ray, neutron diffraction, and electron diffraction) have the ability to characterize crystalline phases [9].

The crystalline phase determines the spatially homogeneous, equilibrium state of a substance [10]. The advantages of X-ray analysis are that the substance is examined in an unchanged state and the results of the analysis determine of the substance and its constituents. Furthermore, X-rays examine the crystal—i.e., the connection itself—and in the case of polymorphic bodies, X-rays make it possible to distinguish between individual modifications inherent in a given substance. A crystal, particularly those of certain chemical compositions, may change its properties due to a phase transformation or distortion of its crystalline structure in response to external or internal physical stress (e.g., mechanical, thermal, etc.) [11,12].

Diffraction methods reveal the slightest changes in the atomic lattice of a crystal that are not captured by other methods. X-ray phase analysis directly examines a particular phase that is present in a sample. This method is rapid, nondestructive, and does not require a large amount of the sample. X-ray phase analysis can also estimate the relative amount of the phase in the mixture (quantitative phase analysis) [13,14]. This method is one of the most used for this research due to many materials, both natural and synthetic, used in advanced technologies are often in a polycrystalline state; therefore, quantitative phase analysis becomes a critical method with which to study their structure and properties.

Quantitative phase analysis can extract a variety of information from a single diffraction pattern. In addition to X-ray fluorescence analysis (XRFA), the quantitative X-ray diffraction analysis of powder materials is widely used in materials science to study the mineral composition of raw materials and finished products, to study phase transformations in materials at different stages of production, and to determine the parameters of lattice parameters [15]. In addition, it has been used in other branches of materials science, such as in glass production [16]. This type of analysis has become vital in the manufacturing and production of raw materials into their final product. For example, whether or not it is feasible, or profitable, to develop a new extraction site at an existing quartzite deposit is largely determined by the mineral's composition.

Understanding the response of quartzite to different temperatures will impact, for example, the technology and equipment required for the preliminary preparation of the raw quartzite as well as for the final product, which may then be intended for further operation under different environmental conditions and temperatures [17]. The active development of 'solar energy' has made characterizing quartzite's properties particularly relevant as this research is needed to discover new deposits of quartzite and enhance its use in the manufacturing of solar cells [18,19].

In addition, quartzite finds application in glass production [16–18]. Its active use for the manufacture of solar cells justifies the increased need for research to discover new deposits of quartzite, which, under the influence of temperatures, would provide the necessary properties [19–21].

The authors in articles [22–25] carried out studies for materials based on Si. Thus, In [22] reported a general bottom-up synthesis of CuO-based trimetallic oxide mesocrystals using a simple precipitation method followed by a hydrothermal treatment and a topotactic transformation via calcination. In [23], CuO catalysts with atomically dispersed co-promoters of Sn and Zn were designed and synthesized. Paper [24] demonstrates a practical route for designing sophisticated architectural structures that combine several structural functions within one catalyst system and their catalysis applications. Work [25] deepens the fundamental understanding of the hydrochlorination of silicon reaction and provides an avenue for the synthesis of Si-based alloy catalysts.

Thus, the purpose of the work is to study quartzite, which is widely used for lining melting furnaces and in the production of dinas, as well as to determine the dependence of changes in the structural parameters of quartzite during heating. The novelty of the work lies in the establishment of structural changes in the material occurring at the studied temperatures using a diffractometer Bruker D8 ADVANCE.

The study of the properties of quartzite for water absorption, open porosity, and apparent density should be carried out at room temperature. The macrostructure and microstructure were investigated before and after firing at a temperature of 1450 °C using optical microscopes, and the phase composition is studied using X-ray diffractometers [26]. For a complete analysis of the presence of impurities in quartzite, a set of the following methods is used: X-ray fluorescence, semiquantitative and quantitative atomic emission, plasma and electrothermal atomic absorption, spectrophotometric, plasma photometric, and semiquantitative and quantitative mass spectrometry with inductively coupled plasma.

A detailed study of quartzite was carried out by Fenner [27], who published a diagram of a one-component system SiO_2 (Figure 1a), which suggested that the changes in quartzite while it was heated to 870 °C were insignificant and that refractory production would not be affected. This was also noted in [28–30].

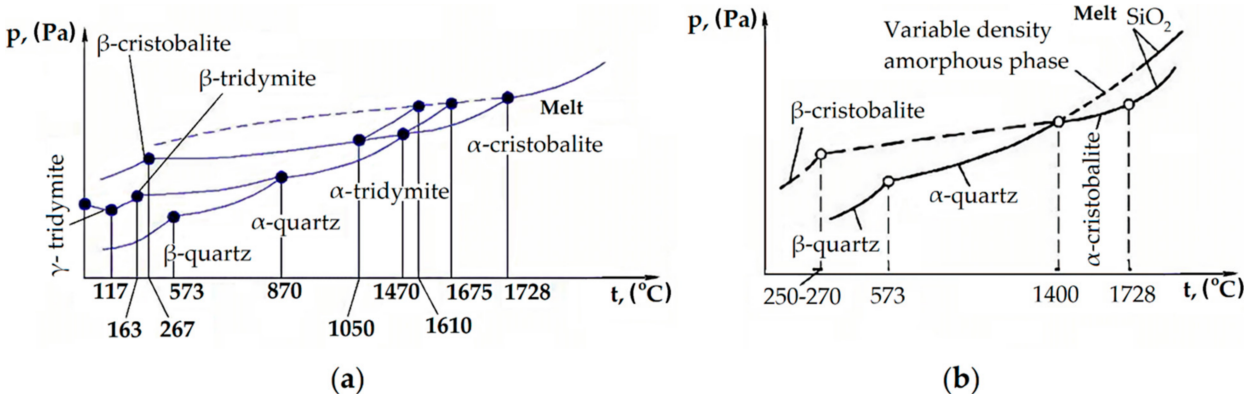


Figure 1. One-component system—SiO_2: (**a**) Fenner diagram; (**b**) Pryanishnikov diagram.

Vapor pressure curves of various modifications of SiO_2 were plotted, and for each given temperature, the lower the vapor pressure curve was (i.e., the curve was closer to the ordinate), the more stable the resultant modification was. However, Fenner's research and physicochemical analysis had not been wholly accurate. Using X-ray structural analysis, scientists in the 1960s and 1970s revised Fenner's conclusions, which had been based on his study of pure silica [31]. Advances in technology and research methods allowed Pryanishnikov to develop a modified diagram of the SiO_2 system (Figure 1b).

The main difference was the elimination of tridymite for pure silica (the number of impurities was not more than 0.01%) [4,6,32]. His diagram, as well as the research of others, revealed that the first transformation of quartz was cristobalite [32–34]. Microscopic studies have also shown that the transformation of quartz into cristobalite occurs at the surface of the grains, in large grains (2–3 mm), and along cracks formed during heat treatment. The front of the phase formation of cristobalite exactly copies the shape of the quartz grain.

There are various data in the literature on the temperature of transformation of α—quartz into cristobalite. It has been indicated that the transformation of quartz into cristobalite requires long exposure and an initial temperature of at least 1000 °C, and its transformation intensifies at 1250–1450 °C [35,36]. The initial transformation temperature also depends on the state of the silica, as the temperature can be relatively low (up to 900 °C) for silicic acid but much higher (up to 1200 °C) for rock crystal. This is also influenced by the impurities contained in the quartzite [37,38].

2. Materials and Methods

This study used Pervouralsk quartzite brand PKMVI-1 with humidity 3% (at temperatures of 25, 70, 100, 110, 200, 400, 600, 879, 1000, 1200, 1470, and 1550 °C), which had the following chemical composition: SiO_2, not less than 97.5%; Al_2O_3, no more than 1.3%, and Fe_2O_3, no more than 0.6%. Grain composition and mass fraction:

- The remainder of the grid No. 2, including 8–14;
- Balance on the grid No. 3.2, no more than 5;
- Passage through the mesh No. 05, including 46–51; and
- Passage through the grid number 01, including 27–32.

This mineral is typically used for the lining of induction melting furnaces [7]. For this study, a Bruker D8 Advance diffractometer with Bragg–Brentano focusing with a high-temperature HTK 16 camera was used. An X-ray tube with a copper anode was used, and the diffraction pattern was recorded with a VÅNTEC-1 high-speed position-sensitive detector with step 0.007°, time for one measurement was 1 h [8].

During the study, a survey was carried out with subsequent printing of a diffraction pattern, which provided information about the parameters of quartzite. In addition, the software of the device gave a decoding of the values of interplanar distances with the selection of the detected elementary cells. Based on this information, the average values of interplanar distances d_{avg}, unit cell volume V_{avg}^3, unit cell density D_{avg}, and molecular

weight M_{avg}, unit cell volume V_{avg} = 115.4 Å^3, unit cell density D_{avg} = 2.590 g/cm^3, and molecular weight M_{avg} were determined. During the study, seven different elementary cells were identified, the cards of which with their characteristics are shown in Table 1.

Table 1. Characteristics of quartzite Pattentov phases identified.

Indicators	Pattent: 00-012-0708 SiO_2 Silicon Oxid Quartz Hexagonal P3221 (154)	Pattent: 01-070-7344 SiO_2 Silicon Oxid Quartz Hexagonal P3221 (154)	Pattent: 01-083-2187 SiO_2 Silicon Oxid Quartz Hexagonal P3221 (152)	Pattent: 01-074-1811 SiO_2 Silicon Oxid Quartz Hexagonal P3221 (152)	Pattent: 01-071-0911 SiO_2 Silicon Oxid Quartz Hexagonal P6222 (180)	Pattent: 01-085-0621 SiO_2 Silicon Oxid Cristobalite Cubic P213 (198)	Pattent: 00-018-1170 SiO_2 Silicon Oxid Tridymite Monoclinic Cc (9)
a, (Å)	4.994	4.916	4.965	4.965	5.0	7.16	18.504
b, c, (Å)	5.438	5.406	5.424	5.424	5.49	-	-
Mol. Weight, (g/mol)	60.08	60.08	60.08	60.08	52.87	60.08	60.08
Volume, (Å^3)	117.45	113.09	115.79	115.79	118.86	367.06	2215.08
D_x, (g/cm^3)	2.548	2.647	2.580	2.580	2.216	2.174	2.254
b, (Å)	-	-	-	-	-	-	5.006
c, (Å)	-	-	-	-	-	-	23.845

To determine the average values of quartzite parameters at each temperature, the values of interplanar distances with a content of at least 5% were selected. Table 2 shows the percentage of varieties of elementary cells of quartzite at each shooting temperature.

Table 2. Content of elementary cells in quartzite at different heating temperatures.

Temperature, °C	00-012-0708	01-070-7344	01-071-0911	01-083-2187	01-074-1811	01-085-2621	00-018-1170
25	58	43	-	-	-	-	-
70	68	32	-	-	-	-	-
100	67	33	-	-	-	-	-
130	69	31	-	-	-	-	-
200	5	10	10	75	-	-	-
400	7	15	12	-	66	-	-
600	9	-	85	7	-	-	-
879	10	-	86	-	-	5	-
1000	12	-	84	-	-	4	-
1200	-	-	96	-	-	4	-
1470	-	-	90	-	-	10	-
1550	-	-	16	-	-	45	39

The calculated averaged values of quartzite parameters at all study temperatures are shown in Table 3.

The diffraction pattern obtained at a temperature of 25 °C showed that the lattice consisted of two varieties of quartzite cells, which had the following characteristics: average interplanar distance d_{avg} = 2.676 Å [19], unit cell volume V_{avg} = 115.4 Å^3, unit cell density D_{avg} = 2.59 g/cm^3, and molecular weight M_{avg} = 60.08 g/mol.

At a temperature of 70–130 °C minor changes occur in the percentage of these cells, which had the following characteristics at temperature 130 °C: average interplanar distance d_{avg} = 2.852 Å, volume V_{avg} = 116.11 Å^3, volume D_{avg} = 2.578 g/cm^3, and molecular weight M_{avg} = 60.08 g/mol.

Table 3. Table of values change of the structural parameters of quartzite during heating.

Lattice Parameters	Temperature °C												
	25	**70**	**100**	**120**	**130**	**200**	**400**	**600**	**879**	**1000**	**1200**	**1470**	**1550**
d_{avg}, Å	2.676	2.77	2.821	2.840	2.852	2.908	2.983	2.988	3.012	3.092	2.997	3.098	3.262
(the change, %)		3.5	5.6	6.1	6.6	8.68	11.5	11.68	12.5	11.55	11.20	11.58	12.19
V_{avg}, Å^3	115.4	116.0	116.0	116.07	116.11	116.55	116.82	118.53	129.85	129.51	129.85	142.48	1020.55
(the change, %)		0.58	0.52	0.58	0.61	0.99	1.23	2.7	12.5	12.2	12.5	23.4	784.36
D_{avg}, g/cm^3	2.590	2.579	2.581	2.579	2.578	2.552	2.547	2.239	2.249	2.258	2.214	2.212	2.212
(the change, %)		−0.43	−0.45	−0.46	−0.47	−1.5	−1.67	−13.5	−13.2	−1.7	−14.5	−14,6	−14.6
M_{avg}, g/mol	60.08	60.08	60.08	60.08	60.08	59.4	59.2	53.9	53.89	54.03	53.18	53.56	50.96
(the change, %)						−1.15	−1.47	−10.3	−10.7	−10.1	−11.5	−10.9	−15.2

At a temperature of 200 °C, shows the appearance of the new cells, characterized by the cards 01-083-2187 and 01-071-0911 and the quartzite structure had the following characteristics: average interplanar distance d_{avg} = 2.909 Å, volume V_{avg} = 116.55 Å^3, volume D_{avg} = 2.552 g/cm^3, and molecular weight M_{avg} = 59.4 g/mol.

At a temperature of 400 °C, appears a new unit cell (01-074-1811) and the structure of quartzite had the following characteristics: average interplanar spacing d_{avg} = 2.983 Å, volume V_{avg} = 116.82 Å^3, volume D_{avg} = 2.547g/cm^3, and molecular weight M_{avg} = 59.2 g/mol.

At a temperature of 600 °C, it showed a significant increase in the content of cells 01-071-0911 [34], and the lattice had the following characteristics: average interplanar distance d_{avg} = 2.989 Å, volume V_{avg} = 118.53 Å^3, volume D_{avg} = 2.239 g/cm^3, and molecular weight M_{avg} = 53.9 g/mol.

3. Results

The diffractogram taken at 879 °C, shown in Figure 2, showed that the number of cells characterized by card 00-012-0708 was 9.53% and 01-071-0911 with M = 52.87 g/mol in an amount of 85.92%, and cristobalite appeared (card 01-085-0621), having M = 60.08 g/mol in an amount 4.55%, V = 367.06 Å^3, D = 2.174 g/cm^3 and size a = 7.16 Å.

The structure characterized by the 01-083-2187 card was absent and the cell had the following characteristics: averaged interplanar distance d_{avg} = 3.013 Å, volume V_{avg} = 129.85 Å^3, volume D_{avg} = 2.234 g/cm^3, and molecular weight M_{avg} = 53.89 g/mol.

At a temperature of 1000 °C, shown in Figure 2b, the number of crystallites characterized by card 00-012-0708 was 12.06%, and 01-071-0911 with M = 52.87 g/mol in an amount of 83.9%, and cristobalite (card 01-085-0621) with M = 60.08 g/mol in the amount of 4.04%. The structure of quartzite had the following characteristics: average interplanar spacing d_{avg} = 3.082 Å, density V_{avg} = 128.51 Å^3, volume D_{avg} = 2.258 g/cm^3, and molecular weight M_{avg} = 54.03 g/mol (Figure 2b).

Figure 2c shows a diffractogram of quartzite taken at 1200 °C. Cells characterized by card 00-012-0708 were not observed, and cells (card 01-071-0911) with M = 52.87 g/mol were 95.57%, and cristobalite (card 085-0621), which has M = 60.08 g/mol, in an amount of 4.43%. The structure of quartzite had the following characteristics: average interplanar spacing d_{avg} = 2.988 Å, V_{avg} = 129.85 Å^3, volume D_{avg} = 2.221 g/cm^3, and molecular weight M_{avg} = 53.18 g/mol.

The diffractogram taken at 1470 °C, shown in Figure 2d, showed that the number of crystals characterized by card 071-0911 with M = 52.87 g/mol was 90.48%, and cristobalite (card 085-0621) having M = 60.08 g/mol in the amount of 9.52%. The structure of quartzite had the following characteristics: average interplanar spacing d_{avg} = 3.098 Å, volume V_{avg} = 142.48 Å^3, volume D_{avg} = 2.212 g/cm^3, and molecular weight M_{avg} = 53.56 g/mol.

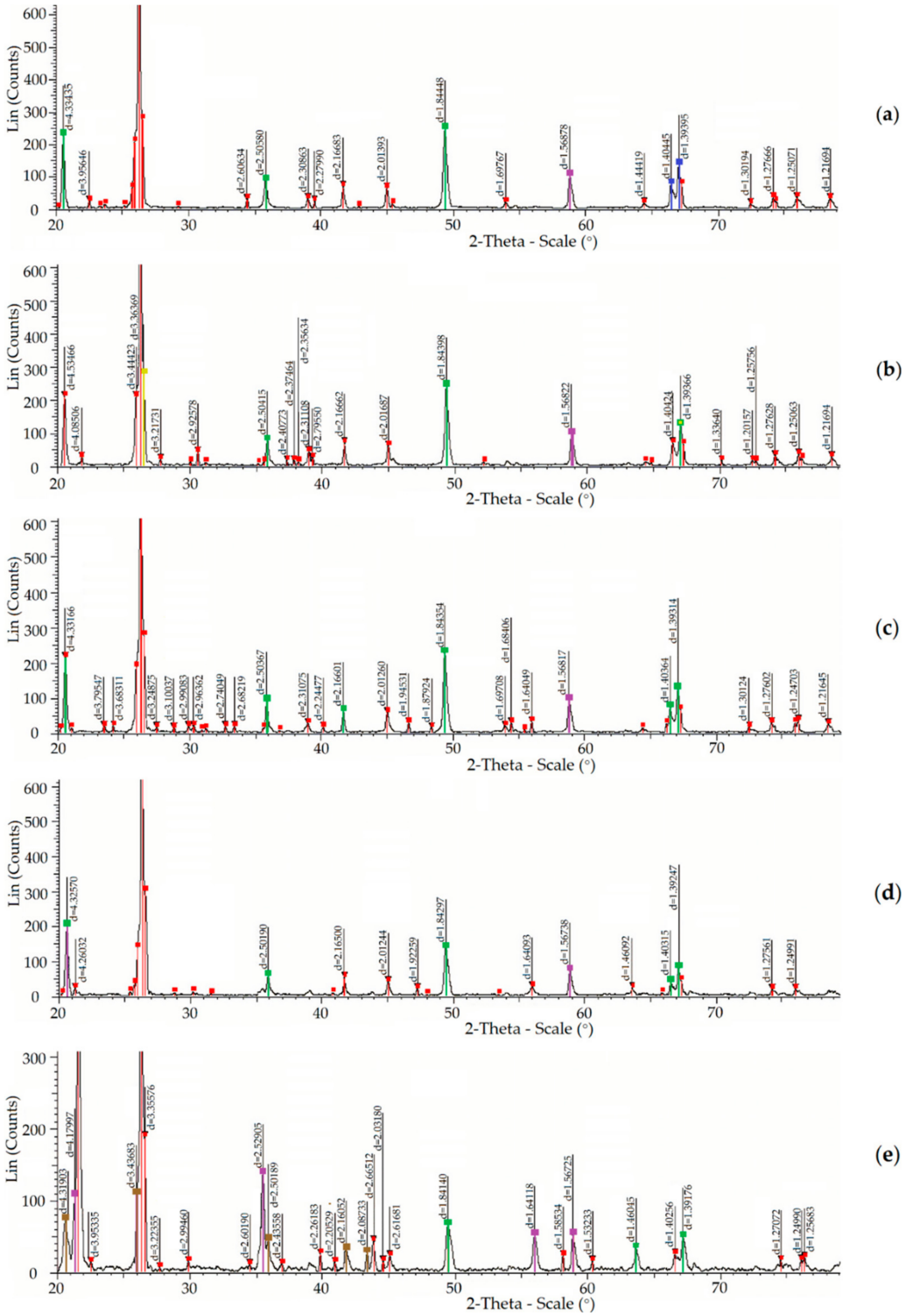


Figure 2. Diffraction pattern of quartzite taken at, where: (**a**) 879 °C, characterizing the appearance of cristobalite with a = 7.16 Å; (**b**) 1000 °C; (**c**) 1200 °C. There are no cells characterized by card 00-012-0708; (**d**) 1470 °C shows a further increase in the cristobalite content; (**e**) 1550 °C. Tridymite cells appeared a = 18.504 Å, b = 5.0064 Å and c = 23.845 Å.

At a temperature of 1550 °C (Figure 2e), there was a further increase in the proportion of cristobalite cells (card 01-085-0621) to 44.69%, a decrease in the proportion of quartzite cells to 15.87%, and tridymite cells appeared (card 00-018-1170) with M = 60.08 g/mol, V = 2125.08 $Å^3$, D = 2.254 g/cm^3 in the amount of 39.43%. The structure of quartzite had the following characteristics: average interplanar spacing d_{avg} = 3.262 Å,

volume V_{avg} = 1020.55 Å^3, volume D_{avg} = 2.212 g/cm^3, and molecular weight M_{avg} = 50.96 g/mol.

Based on the data obtained, the dependence of changes in the structure parameters of quartzite, grade PKMVI-1, was constructed (Figure 3a), and a new version of the scheme of transformations of this quartzite at normal pressure was proposed (Figure 3b, scheme of transformations of quartzite grade at normal pressure).

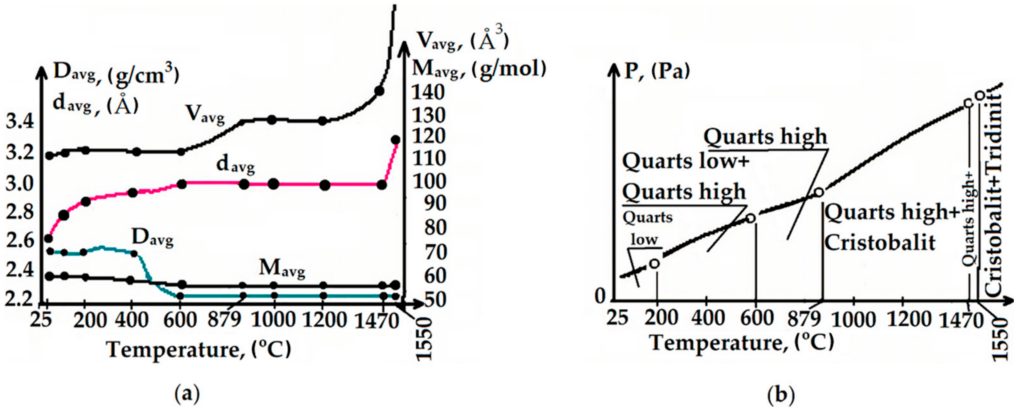


Figure 3. Dependences of changes in the structural parameters of quartzite upon heating: (**a**) dependence of changes in the averaged values V_{avg}, M_{avg}, d_{avg}, and D_{avg} from temperature; (**b**) scheme of transformations of quartzite grade PKMVI-1 at normal pressure for crystalline modifications.

Heating from 25 to 200 °C led to changes in interplanar distance d_{avg}, the values V_{avg}, M_{avg}, and D_{avg} did not change, and the structure of quartzite consisted of a crystalline modification Quartz low. The d_{avg} value changed by 5.2%, as compared to the initial value. At this time, the process of drying took place.

In the range of 200–400 °C, the d_{avg} value continued to change and its difference at 400 °C was 3%. The drying process continued, and in addition to the crystalline modification Quartz low, the crystalline modification Quartz high appeared in the structure of quartzite. For this reason, a slight change in the molecular weight M_{avg} was observed.

Further heating from 400 to 600 °C led to a continuing increase in interplanar spacings and a sharp decrease in density D_{avg} as well as a significant decrease in molecular weight M_{avg} (to 10%). At temperatures above 600 °C, the structure of quartzite consisted only of the crystalline modification Quartz high, and up to 879 °C, there was a sharp increase in the volume of the unit cell V_{avg} while other parameters underwent minor changes.

From 879 to 1470 °C, the process of the appearance of the crystalline modification of cristobalite was underway, which to minor changes in the structural parameters.

Above 1470 °C, there was a sharp increase in values D_{avg} (by 14%) and V_{avg} (by 784%), which led to the appearance of a crystalline modification tridymite.

4. Conclusions

As a result of the study, the averaged values were determined for V_{avg}, M_{avg}, d_{avg}, and D_{avg} at the temperatures 25, 70, 100, 110, 200, 400, 600, 879, 1000, 1200, 1470, and 1550 °C, and they were plotted according to their dependence upon heating (Figure 3a).

On the basis of the data obtained, a refined scheme of transformations of quartzite grade PKMVI-1 at normal pressure for crystalline modifications was proposed. This research found that, at temperatures up to 200 °C, the lattice consisted of a crystalline modification Quartz low, from 200 to 600 °C of Quartz low + Quartz high, from 600 to 879 °C contained only Quartz high, and from 879 to 1470 °C from Quartz high and cristobalite, and finally, from 1470 to 1550 °C, the structure consisted of modifications Quartz high, cristobalite, and tridymite.

Therefore, the authors found that tridymite, for a given quartzite, appeared only at a temperature of 1470 °C. This research has made it possible to establish the nature of changes

in the structural parameters of quartzite at temperatures ranging from 25 to 1550 °C, which are presented in Table 3.

As a result of this research, the changes in such parameters of the lattice parameter can be seen, such as the average interplanar distance d_{avg}, the volume of the unit cell V_{avg}, the density of the unit cell D_{avg}, and the molecular weight M_{avg}. This research disagreed with previous reports that tridymite formed when heated to 1200–1470 °C. It was found that in the temperature range 200–600 °C, there was a sharp decrease in molecular weight (up to 10%), which was explained by the appearance of the crystalline modification Quartz high. The appearance of cristobalite did not lead to abrupt changes in the lattice parameters. The formation of the crystalline modification tridymite was accompanied by an abrupt change in the unit cell volume V_{avg} (by 780%) and molecular weight M_{avg} (by 15%).

The proposed scheme for the transformation of quartzite showed, in more detail, the changes in the parameters of its lattice during heating and provided a rationale for the choice in technology for drying as well as for obtaining tridymite when this material is used for the manufacture of thermal unit lining.

Author Contributions: Conceptualization, V.A.K., A.I.C. and V.S.T.; Data curation, V.A.K., A.I.C., V.V.K., V.S.T., V.V.B. and R.B.S.; Formal analysis, V.A.K., A.I.C., V.V.K., V.S.T., A.M.P. and S.V.T.; Investigation, V.A.K., A.I.C., V.V.K., V.S.T., V.V.B., A.M.P. and R.B.S.; Methodology, V.A.K., V.V.K., A.M.P. and S.V.T.; Project administration, V.A.K., A.I.C. and V.S.T.; Resources, V.A.K. and V.V.B.; Software, V.V.B.; Supervision, V.A.K., A.I.C. and V.S.T.; Validation, A.I.C., V.V.K., V.S.T., V.V.B., A.M.P., R.B.S. and S.V.T.; Visualization, V.V.K., V.V.B., R.B.S. and S.V.T.; Writing—original draft, V.A.K., A.I.C., V.V.K., V.S.T., V.V.B., A.M.P., R.B.S. and S.V.T.; Writing—review and editing, V.A.K., A.I.C., V.V.K., V.S.T., V.V.B., A.M.P., R.B.S. and S.V.T. All authors have read and agreed to the published version of the manuscript.

Funding: The studies were carried out according to the state assignment from the Ministry of Science and Higher Education of the Russian Federation for the project "Development of a set of scientific and technical solutions in the field of creating biofuels and optimal biofuel compositions, providing the possibility of transforming consumed types of energy in accordance with trends in energy efficiency, reducing the carbon footprint of products and using alternative fuels to fossil fuels" (Contract FSRZ-2021-0012) in the scientific laboratory of biofuel compositions of the Siberian Federal University, created as part of the activities of the Scientific and Educational Center "Yenisei Siberia".

Institutional Review Board Statement: Not applicable.

Informed Consent Statement: Not applicable.

Data Availability Statement: Not applicable.

Conflicts of Interest: The authors declare no conflict of interest.

References

1. Jung, L. *High Purity Natural Quartz*; Qua Technology Inc.: Liberty Corner, NJ, USA, 1992; p. 657.
2. Kondratyev, E.A.; Gorbunov, V.V. Expansion of the range and creation of high-quality import-substituting refractory products. *Metallurgist* **2015**, *3*, 11–14.
3. Bereznyak, E.P.; Kolodiy, I.V.; Khodyreva, Y.S. The Effect of The External Medium On The Structural-phase Transformations of Quartzite Upon High-Energy Electron Irradiation. *Vopr. At. Nauk. Tekhniki* **2019**, *123*, 30–34. [CrossRef]
4. Miras, A.; Galán, E.; González, I.; Romero-Baena, A.; Martín, D. Mineralogical evolution of ceramic clays during heating. An ex/in situ X-ray diffraction method comparison study. *Appl. Clay Sci.* **2018**, *161*, 176–183. [CrossRef]
5. Kukartsev, V.A. Application of Pervouralsky quartzite in acidic lining for induction iron-melting furnaces. *Foundry Russ.* **2012**, *2*, 35.
6. Pryanishnikov, V.P. *Silica System*; Stroyizdat: Saint Petersbourgh, Russia, 1971.
7. Mitra, S. Kinetics of quartz transformation. *Trans. Indian Ceram. Soc.* **2014**, *33*, 25–38. [CrossRef]
8. Kukartsev, V.A.; Abkaryan, A.K. Study by X-ray methods of the effect of temperature on crystal lattice interplanar distances of Pervoural'sk quartzite used for induction furnace lining. *Refract. Ind. Ceram.* **2014**, *54*, 413–415. [CrossRef]
9. Nagurney, A.B.; Caddick, M.J.; Law, R.D.; Ross, N.L.; Kruckenberg, S.C. Crystallographically controlled void space at grain boundaries in the Harkless quartzite. *J. Struct. Geol.* **2021**, *143*, 142–154. [CrossRef]
10. Benmore, C.J. A Review of High-Energy X-ray Diffraction from Glasses and Liquids. *ISRN Mater. Sci.* **2012**, *11*, 852905. [CrossRef]
11. Cartwright, J.H.; García-Ruiz, J.M.; Piro, O.; Sainz-Díaz, C.I.; Tuval, I. Chiral symmetry breaking during crystallization: An advection-mediated nonlinear autocatalytic process. *Phys. Rev. Lett.* **2004**, *93*, 035502. [CrossRef]

12. Szurgot, M. Investigations of Impurity Striations in Potassium Bichromate Crystals. *Cryst. Res. Technol.* **2010**, *45*, 347–354. [CrossRef]
13. Proffen, T.; Page, K.L.; McLain, S.E.; Clausen, B.; Darling, T.W.; TenCate, J.A.; Lee, S.-Y.; Ustundag, E. Atomic pair distribution function analysis of materials containing crystalline and amorphous phases. *Z. Krist.-Cryst. Mater.* **2005**, *220*, 1002–1008. [CrossRef]
14. Biswas, R.K.; Khan, P.; Mukherjee, S.; Mukhopadhyay, A.K.; Ghosh, J.; Muraleedharan, K. Study of short range structure of amorphous Silica from PDF using Ag radiation in laboratory XRD system, RAMAN and NEXAFS. *J. Non-Cryst. Solids* **2018**, *488*, 1–9. [CrossRef]
15. Kim, S.J.; Choi, J.H.; Lee, S.C.; Park, C. Effects of temperature and tilt angle on the grain boundary structure in silicon oxide: Molecular dynamics study. *Met. Mater. Int.* **2010**, *16*, 163–169. [CrossRef]
16. An Kihara, K. An X-ray study of the temperature dependence of the quartz structure. *Eur. J. Mineral.* **1990**, *2*, 63–78. [CrossRef]
17. Skamnitskaya, L.; Bubnova, T. Mineralogi-technological evaluation of Girvas occurrence vein quartz. *Int. Multidiscip. Sci. Geoconf. SGEM* **2019**, *19*, 877–882. [CrossRef]
18. Shimura, T.; Fukuda, K.; Yasutake, K.; Hosoi, T.; Umeno, M. Comparison of ordered structure in buried oxide layers in high-dose, low-dose, and internal-thermal-oxidation separation-by-implanted-oxygen wafers. *Thin Solid Film.* **2005**, *476*, 125–129. [CrossRef]
19. Ananiev, Y.S.; Ananyeva, L.G.; Dolgov, I.V.; Korobeinikov, A.F.; Korovkin, M.V. Search, evaluation and enrichment of quartz raw materials for high technologies. *Bull. Tomsk Polytech. Univ. Georesour. Eng.* **2001**, *304*, 123–130.
20. Sánchez-Borrego, F.J.; Álvarez-Mateos, P.; García-Martín, J.F. Biodiesel and Other Value-Added Products from Bio-Oil Obtained from Agrifood Waste. *Processes* **2021**, *9*, 797. [CrossRef]
21. Yaqoob, H.; Teoh, Y.H.; Sher, F.; Jamil, M.A.; Murtaza, D.; Al Qubeissi, M.; UI Hassan, M.; Mujtaba, M.A. Current Status and Potential of Tire Pyrolysis Oil Production as an Alternative Fuel in Developing Countries. *Sustainability* **2021**, *13*, 3214. [CrossRef]
22. Liu, H.; Ji, Y.; Li, J.; Zhang, Y.; Wang, X.; Yu, H.; Wang, D.; Zhong, Z.; Gu, L.; Xu, G.; et al. A general bottom-up synthesis of CuO-based trimetallic oxide mesocrystal superstructures for efficient catalytic production of trichlorosilane. *Nano Res.* **2020**, *13*, 2819–2827. [CrossRef]
23. Shi, Q.; Ji, Y.; Chen, W.; Zhu, Y.; Li, J.; Liu, H.; Li, Z.; Tian, S.; Wang, L.; Zhong, Z.; et al. Single-atom Sn-Zn pairs in CuO catalyst promote dimethyldichlorosilane synthesis. *Natl. Sci. Rev.* **2020**, *7*, 600–608. [CrossRef] [PubMed]
24. Yang, Z.; Kang, T.; Ji, Y.; Li, J.; Zhu, Y.; Liu, H.; Jiang, H.; Zhong, Z.; Su, F. Architectural Cu2O@ CuO mesocrystals as superior catalyst for trichlorosilane synthesis. *J. Colloid Interface Sci.* **2021**, *589*, 198–207. [CrossRef] [PubMed]
25. Su, K.; Luo, J.; Ji, Y.; Jiang, X.; Li, J.; Zhang, J.; Zhong, Z.; Su, F. Use of the active-phase Cu3Si alloy as superior catalyst to direct synthesis of trichlorosilane via silicon hydrochlorination. *J. Solid State Chem.* **2021**, *304*, 122591. [CrossRef]
26. Nepomnyashchikh, A.I.; Krasin, B.A.; Vasilyeva, I.E.; Eliseev, I.A.; Eremin, V.P.; Fedoseenko, V.A.; Sinitskiy, V.V. Silicon for solar energy. *Bull. Tomsk Polytech. Univ. Georesour. Eng.* **2000**, *303*, 176–190.
27. Fenner, C.N. The various forms of silica and their mutual relations. *J. Wash. Acad. Sci.* **1912**, *2*, 471–480.
28. Thompson, A.B.; Wennemer, M. Heat capacities and inversions in tridymite, cristobalite, and tridymite-cristobalite mixed phases. *Am. Mineral.* **1979**, *64*, 1018–1026.
29. Wenk, H.R.; Barton, N.; Bortolotti, M.; Vogel, S.C.; Voltolini, M.; Lloyd, G.E.; Gonzalez, G.B. Dauphiné twinning and texture memory in polycrystalline quartz. Part 3: Texture memory during phase transformation. *Phys. Chem. Miner.* **2009**, *36*, 567–583. [CrossRef]
30. Ringdalen, E. Changes in Quartz During Heating and the Possible Effects on Si Production. *JOM* **2015**, *67*, 484–492. [CrossRef]
31. Germinario, L.; Andriani, G.F.; Laviano, R. Petrography, mineralogy, chemical and technical properties of the building stone of Ostuni Cathedral (Italy): Inferences on diagnostics and conservation. *Period. Mineral.* **2014**, *83*, 379–400. [CrossRef]
32. Kukartsev, V.A.; Kukartsev, V.V.; Kukartsev, A.V. Effect of the temperature treatment of quartzite on the lining resistance of commercial-frequency induction crucible furnaces. *Refract. Ind. Ceram.* **2018**, *59*, 252–256. [CrossRef]
33. Schneider, H.; Flörke, O.W. High-temperature transformation of tridymite single crystals to cristobalite. *Z. Krist.-Cryst. Mater.* **1986**, *175*, 165–176.
34. Wahl, F.M.; Grim, R.E.; Graf, R.B. Phase transformations in silica as examined by continuous X-ray diffraction. *Am. Mineral. J. Earth Planet. Mater.* **1961**, *46*, 196–208.
35. Kashcheev, I.D.; Strelov, K.K.; Mamykin, P.S. *Chemical Technology of Refractories*; Intermet Engineering: Moscow, Russia, 2007.
36. Zavertkin, A.S. Effect of Quartzite Heat Treatment on Induction Furnace Lining Failure Mechanism. *Refract. Ind. Ceram.* **2019**, *60*, 67–70. [CrossRef]
37. Shchiptsov, V.V.; Perepelitsyn, V.A.; Grishenkov, E.E.; Enenko, V.P.; Zavertkin, A.S. Pervoural'skii and Karel'skii quartzites for the lining of crucible-type induction furnaces. *Refract. Ind. Ceram.* **2003**, *44*, 67–74. [CrossRef]
38. Kukartsev, V.A.; Abkaryan, A.K.; Temnykh, V.I.; Kukartsev, V.V.; Tynchenko, V.S.; Kukartsev, A.V. Changes in Pervoural Quartzite Crystal Lattice on Heating from 25 to 600 °C. *Refract. Ind. Ceram.* **2021**, *62*, 162–167. [CrossRef]